# PROJECTION BASED EMBEDDING THEORY FOR SOLVING KOHN-SHAM DENSITY FUNCTIONAL THEORY

LIN LIN* AND LEONARDO ZEPEDA-NÚÑEZ†

**Abstract.** Quantum embedding theories are playing an increasingly important role in bridging different levels of approximation to the many body Schrödinger equation in physics, chemistry and materials science. In this paper, we present a linear algebra perspective of the recently developed projection based embedding theory (PET) [Manby et al, J. Chem. Theory Comput. 8, 2564, 2012], restricted to the context of Kohn-Sham density functional theory. By partitioning the global degrees of freedom into a "system" part and a "bath" part, and by choosing a proper projector from the bath, PET is an in principle exact formulation to confine the calculation to the system part only, and hence can be carried out with reduced computational cost. Viewed from the perspective of the domain decomposition method, one particularly interesting feature of PET is that it does not enforce a boundary condition explicitly, and remains applicable even when the discretized Hamiltonian matrix is dense, such as in the context of the planewave discretization. In practice, the accuracy of PET depends on the accuracy of the projector for the bath. Based on the linear algebra reformulation, we develop a first order perturbation correction to the projector from the bath to improve its accuracy. Numerical results for real chemical systems indicate that with a proper choice of reference system, the perturbatively corrected PET can be sufficiently accurate even when strong perturbation is applied to very small systems, such as the computation of the ground state energy of a $SiH_3F$ molecule, using a $SiH_4$ molecule as the reference system.

**1. Introduction.** Multiphysics simulation usually involves two or more physical scales. In the context of the electronic structure theory, even though everything is described by the many body Schrödinger equation on the scale of electrons and molecules, it turns out that the concept of multiphysics simulation remains valid. The direct solution to the many body Schrödinger equation itself is prohibitively expensive, except for systems with a handful of electrons. This has led to the development of various theoretical tools in both quantum physics and quantum chemistry to find approximate solution to the Schrödinger equation. These theories can be effectively treated as "different levels of physics" providing different levels of accuracy. However, depending on the accuracy required, the computational cost associated with such approximate theories can still be very high. So if a large quantum system can be partitioned into a "system" part containing the degrees of freedom that are of interest that need to be treated using a more accurate theory, and a "bath" part containing the rest of the degrees of freedom that can be treated using a less accurate theory, it becomes naturally desirable to have a numerical method that can bridge the two levels of theories. In quantum physics, such "multiscale" methods have been actively developed in the past few decades and are often called "quantum embedding theories" (see *e.g.* [7, 19, 13, 15, 11, 4, 2, 35, 33, 18, 36, 17, 28, 5, 23] and [31] for a recent brief review).

The projection based embedding theory (PET) [26] is a recently developed quantum embedding theory, which is a versatile method that can be used to couple a number of quantum theories together in a seamless fashion (also see recent works [24, 6]). This paper is a first step towards a mathematical understanding PET. To make the discussions concrete, we assume that the system part is described by the widely used Kohn-Sham density functional theory (KSDFT) [14, 22], and the bath part is also

*Department of Mathematics, University of California, Berkeley, Berkeley, CA 94720 and Computational Research Division, Lawrence Berkeley National Laboratory, Berkeley, CA 94720. Email: linlin@math.berkeley.edu

†Computational Research Division, Lawrence Berkeley National Laboratory, Berkeley, CA 94720. Email: lzepeda@lbl.gov

described by KSDFT but is solved only approximately. Although this setup is simpler than that in [26], it is already interesting from the perspective of approximate solution of large scale eigenvalue problems, as to be detailed below.

After proper discretization, KSDFT can be written as the following nonlinear eigenvalue problem

$$H[P]\Psi = \Psi\Lambda, \quad P = \Psi\Psi^*, \tag{1.1}$$

where $H[P] \in \mathbb{C}^{N\times N}$ is a Hermitian matrix, and the diagonal matrix $\Lambda \in \mathbb{R}^{N_e\times N_e}$ encodes the algebraically lowest $N_e$ eigenvalues ($N \gg N_e$). $N$ is the number of degrees of freedom of the Hamiltonian operator after discretization, and $N_e$ is the number of electrons in the system (spin degrees of freedom omitted). The eigenvectors associated with $\Lambda$ are denoted by $\Psi = [\psi_1, \ldots, \psi_{N_e}] \in \mathbb{C}^{N\times N_e}$, and $\Psi$ satisfies the orthonormality condition $\Psi^*\Psi = I_{N_e}$. The matrix $P$ is a spectral projector, usually called the *density matrix*. The Hamiltonian $H[P]$ depends on the density matrix $P$ in a nonlinear fashion, and Eq. (1.1) needs to be solved self-consistently. Without loss of generality, the system part can be defined as the degrees of freedom associated with a set of indices $\mathcal{I}_s$, and the bath part with a set of indices $\mathcal{I}_b$, so that $\mathcal{I}_s \cup \mathcal{I}_b = \{1, \ldots, N\}$. Usually $|\mathcal{I}_b| \gg |\mathcal{I}_s|$, and it is possible that $\mathcal{I}_s \cap \mathcal{I}_b \neq \emptyset$. We are mostly interested in the accurate computation of physical observables associated with the system part, *i.e.* the matrix block of the density matrix $P_{\mathcal{I}_s,\mathcal{I}_s}$. Since the eigenvalue problem (1.1) couples all degrees of freedom together, this task still requires a relatively accurate description of the rest of the matrix blocks of the density matrix.

In a nutshell, PET assumes the following decomposition of the density matrix

$$P = P_s + P_{0,b}, \tag{1.2}$$

in which $P_s$ is the density matrix corresponding to the system part whose block corresponding to the bath part, $(P_s)_{\mathcal{I}_b,\mathcal{I}_b}$, approximately vanishes. Similarly $P_{0,b}$, called the reference projector, is the density matrix from the bath part whose block corresponding to the system part, $(P_{0,b})_{\mathcal{I}_s,\mathcal{I}_s}$, approximately vanishes. The decomposition of the system and bath part is performed using projectors, thus leading to the name of PET. Such a decomposition can be *in principle exact*. The subscript 0 indicates that $P_{0,b}$ is fixed and is only obtained approximately. Furthermore, $P_s$ is constrained by $P_{0,b}$ according to the orthogonality condition

$$P_{0,b}P_s = 0. \tag{1.3}$$

The condition (1.3) acts as a soft "boundary condition" for a modified Kohn-Sham problem, of which the number of eigenvectors to be computed can be much smaller than $N_e$. Hence PET reduces the computational cost compared to Eq. (1.1) by reducing the number of eigenvectors and eigenvalues to compute.

**Related works:**

From a practical perspective, one alluring advantage of PET is that it only requires the matrix-vector multiplication operation of the form $H\psi$, thus it can be applicable even when $H$ is a dense matrix such as in the planewave discretization. This advantage it makes it suitable to be naturally utilized in many electronic structure software packages. This is in contrast to *e.g.* , the widely used Green's function embedding method (see *e.g.* [2, 35, 33, 18, 23]), which requires that $H$ to be a sparse matrix. However, when $H$ is indeed sparse, Green's function embedding method may achieve lower complexity than PET [23], and it may perform better for systems with small gaps.

**Contribution:**

The contribution of this paper is two-fold: First, we provide a mathematical understanding of PET from a linear algebra perspective, which can be concisely stated as an energy minimization problem with a constrained domain. The corresponding Euler-Lagrange equation from the energy minimization problem gives rise to a modified Kohn-Sham problem, and the original PET formulation can be understood as a penalty method for implementing the orthogonality constraint (1.3). We then extend the formalism to the nonlinear case as in KSDFT. Second, we derive a perturbation formula for obtaining the first order correction to the density matrix. We find that such a first order correction to the system part of the density matrix automatically vanishes, and the perturbative correction is then only used to correct the bath part of the density matrix.

Our numerical results for real chemical systems confirm the effectiveness of the method. In particular, we find that the method can reach below the chemical accuracy (1 kcal/mol, or 0.0016 au) even when applied to very small systems, such as the computation of the ground state energy of a $SiH_3F$ molecule from the reference of a $SiH_4$ molecule. We also demonstrate the accuracy of the energy and the atomic force for the PET and the perturbatively corrected PET using other molecules such as benzene and anthracene.

**Organization:**

This paper is organized as follows. We derive PET for linear problems in section 2, and introduce the first order perturbative correction to PET in section 3. We then generalize the discussion to nonlinear problems in section 4. We discuss the strategy to evaluate the reference projector using localization methods in section 5. We then present the numerical results in section 6, followed by the conclusion and discussion in section 7.

**2. PET for linear problems.** We first introduce PET in the context of solving a linear eigenvalue problem. Let $H \in \mathbb{C}^{N\times N}$ be a Hermitian matrix, whose eigenvalues are ordered non-decreasingly as $\lambda_1 \le \lambda_2 \le \ldots \le \lambda_{N_e} < \lambda_{N_e+1} \le \ldots \le \lambda_N$. Here we assume that there is a positive energy gap $\Delta_g = \lambda_{N_e+1} - \lambda_{N_e}$.

Consider the following energy minimization problem

$$E = \inf_{\substack{P^2 = P, P^* = P \\ \mathrm{Tr}P = N_e}} \mathcal{E}[P], \tag{2.1}$$

where $E$ is called the energy, and the energy functional $\mathcal{E}[P]$ is defined as

$$\mathcal{E}[P] := \mathrm{Tr}[HP]. \tag{2.2}$$

Note that the condition $P = P^2$ requires $P$ to be a projector, with eigenvalues being either 0 or 1. The trace condition ensures that there are precisely $N_e$ eigenvalues that are equal to 1. Proposition 1 states that the minimizer is attained by solving a linear eigenvalue problem. This is a well known result in linear algebra; nonetheless, we provide its proof here in order to motivate the derivation for PET later.

PROPOSITION 1. *Assume that there is a positive gap between the $N_e$-th and $(N_e+1)$-th eigenvalue of $H$. Then the variational problem (2.1) has a unique minimizer, which is given by the solution to the following linear eigenvalue problem*

$$H\Psi = \Psi\Lambda, \quad P = \Psi\Psi^*. \tag{2.3}$$

*Here $(\Psi, \Lambda)$ are the lowest $N_e$ eigenpairs of $H$.*

*Proof.* Since $H$ is a Hermitian matrix, it can be diagonalized as

$$H = \hat{\Psi}\hat{\Lambda}\hat{\Psi}^*. \tag{2.4}$$

Here $\hat{\Lambda} = \mathrm{diag}[\lambda_1, \ldots, \lambda_N] \in \mathbb{R}^{N\times N}$ is a diagonal matrix containing all the eigenvalues of $H$ ordered non-decreasingly, and $\hat{\Psi} \in \mathbb{C}^{N\times N}$ is a unitary matrix with its first $N_e$ columns given by $\Psi$. Then

$$\mathcal{E}[P] = \mathrm{Tr}[HP] = \mathrm{Tr}[\hat{\Psi}\hat{\Lambda}\hat{\Psi}^* P] = \mathrm{Tr}[\hat{\Lambda}\hat{\Psi}^* P\hat{\Psi}] = \mathrm{Tr}[\hat{\Lambda}\hat{P}] = \sum_{i=1}^{N} \lambda_i \hat{P}_{ii} =: \hat{\mathcal{E}}[\hat{P}], \tag{2.5}$$

where $\hat{P} = \hat{\Psi}^* P \hat{\Psi}$ is the density matrix with respect to the basis given by $\hat{\Psi}$. Thus, Eq. (2.1) is equivalent to

$$E = \inf_{\substack{\hat{P}^2 = \hat{P},\, \hat{P}^* = \hat{P} \\ \mathrm{Tr}\hat{P} = N_e}} \hat{\mathcal{E}}[\hat{P}] \tag{2.6}$$

Since $\lambda_{N_e+1} - \lambda_{N_e} > 0$, the minimizer is achieved by setting

$$\hat{P}_{ii} = \begin{cases} 1, & \text{if } i \le N_e, \\ 0, & \text{if } i > N_e. \end{cases} \tag{2.7}$$

Finally, given that $\hat{P}$ is an idempotent matrix, we have that all its eigenvalues are either 0 or 1. By the Courant-Fischer minimax theorem [12], all diagonal entries $\hat{P}_{ii}$ are already eigenvalues, and $P$ is diagonalized by the identity matrix. Thus $\hat{P}$ is a diagonal matrix, with ones and zeros at the main diagonal, *i.e.*

$$\hat{P}_{ij} = \begin{cases} 1, & \text{if } i = j \text{ and } i \le N_e, \\ 0, & \text{otherwise.} \end{cases} \tag{2.8}$$

This is the unique minimizer. Thus

$$P = \hat{\Psi}\hat{P}\hat{\Psi}^* = \Psi\Psi^*. \tag{2.9}$$

is the unique minimizer of (2.1), where $\Psi$ is given by the first $N_e$ columns of $\hat{\Psi}$. □

When $N$ and $N_e$ are large, the solution of the linear eigenvalue problem (2.3) can be expensive. However, if we have already solved the eigenvalue problem for a reference matrix $H_0$, and we would like to solve the eigenvalue problem for another matrix $H$, so that $H - H_0$ is approximately zero outside the matrix block given by the index set $\mathcal{I}_s$. In such case, PET aims at reducing the computational cost by solving a modified eigenvalue problem that involves a much smaller number of eigenvectors.

More specifically, for a reference system $H_0 \in \mathbb{C}^{N\times N}$, let $P_0$ be the minimizer of the following problem

$$E_0 = \inf_{\substack{P^2 = P,\, P^* = P \\ \mathrm{Tr}P = N_e^0}} \mathrm{Tr}[H_0 P]. \tag{2.10}$$

We split the minimizer as

$$P_0 = P_{0,b} + P_{0,s}. \tag{2.11}$$

where both $P_{0,b}$, and $P_{0,s}$ are projectors themselves, *i.e.* $P_{0,b}^2 = P_{0,b}$, $P_{0,s}^2 = P_{0,s}$, and the rank of $P_{0,b}$ is denoted by $N_b := \mathrm{Tr}P_{0,b}$. We assume that $N_b \approx N_e^0$, and hence

the rank of $P_{0,s}$ is much smaller than $N_b$. The splitting procedure (2.11) is by no means unique; we will discuss one possible method based on localization techniques to choose $\Psi_{0,b}$ in section 5.

Together with $P_0^2 = P_0$, we have

$$P_0^2 = (P_{0,b} + P_{0,s})^2 = P_{0,b}^2 + P_{0,s}^2 + P_{0,b}P_{0,s} + P_{0,s}P_{0,b} = P_{0,b} + P_{0,s}. \tag{2.12}$$

Hence we have the orthogonality condition $P_{0,b}P_{0,s} = 0$. It is also convenient to write

$$P_{0,b} = \Psi_{0,b}\Psi_{0,b}^*, \quad \Psi_{0,b}^*\Psi_{0,b} = I_{N_b}. \tag{2.13}$$

By proper rotation[1] of the $\Psi_{0,b}$ matrix, without loss of generality we may assume that

$$\Psi_{0,b}^* H_0 \Psi_{0,b} := \Lambda_{0,b} \tag{2.14}$$

is a diagonal matrix. We define $\mathcal{B}_0 := \mathrm{span}\{\Psi_{0,b}\}$, with its orthogonal complement denoted by $\mathcal{B}_0^\perp$.

The main ansatz in PET is that the density matrix $P$ can be split as

$$P = P_{0,b} + P_s, \tag{2.15}$$

where $P_s^2 = P_s$ is also a projector, and $P_{0,b}$ is as the reference projector as in (2.11). Similar to the discussion above, we arrive at the orthogonality condition (1.3). Since the rank of $P_{0,b}$ is already $N_b$, the rank of $P_s$ is thus equal to $N_s := N_e - N_b$, and we expect that $N_s \ll N_b$. Note that the dimension of $H_0$ and $H$ must be the same, but $N_e^0$ and $N_e$ can be different. Thus the ranks of $P_{0,s}$ and $P_s$ can also be different. This is necessary in the context of KSDFT, where the system part in $H$ can involve different numbers and/or types of atoms from that in $H_0$.

With the reference projector fixed PET solves the following constrained minimization problem only with respect to $P_s$:

$$E^{\mathrm{PET}} = \inf_{\substack{P_s^2 = P_s,\, P_s^* = P_s \\ P_{0,b}P_s = 0,\, \mathrm{Tr}P_s = N_s}} \mathrm{Tr}[H(P_s + P_{0,b})]. \tag{2.16}$$

Compared to (2.1), we find that PET restrains the domain of the density matrices only to those satisfying the ansatz (2.15). Hence by the variational principle $E^{\mathrm{PET}} \geq E$ provides an upper bound for the energy. Parallel to Proposition 1, the minimizer of (2.16) is uniquely obtained by a modified linear eigenvalue problem. This is given in Proposition 2.

PROPOSITION 2 (Projection based embedding). *Let $H|_{\mathcal{B}_0^\perp}$ be the restriction of $H$ to the subspace $\mathcal{B}_0^\perp$, and assume that there is a positive gap between the $N_s$-th and $(N_s+1)$-th eigenvalue of $H|_{\mathcal{B}_0^\perp}$. Then the variational problem (2.16) has a unique minimizer, which is given by the solution to the following linear eigenvalue problem*

$$H|_{\mathcal{B}_0^\perp}\Psi_s = \Psi_s\Lambda_s, \quad P_s = \Psi_s\Psi_s^*. \tag{2.17}$$

*Here $(\Psi_s, \Lambda_s)$ are the lowest $N_s$ eigenpairs of $H|_{\mathcal{B}_0^\perp}$.*

[1]This can be achieved by solving the eigenvalue problem $\left(\Psi_{0,b}^* H_0 \Psi_{0,b}\right) C_b = C_b \Lambda_{0,b}$, and redefining $\Psi_{0,b}$ to be $\Psi_{0,b}C_b$.

*Proof.* First, the orthogonality condition $P_{0,b}P_s = 0$ implies that all columns of $P_s$ should be in the subspace $\mathcal{B}_0^\perp$. Using the relation

$$\begin{aligned}\mathrm{Tr}[(I-P_{0,b})H(I-P_{0,b})P_s] &= \mathrm{Tr}[HP_s - HP_{0,b}P_s - P_{0,b}HP_s + P_{0,b}HP_{0,b}P_s],\\ &= \mathrm{Tr}[HP_s - HP_{0,b}P_s - HP_sP_{0,b} + HP_{0,b}P_sP_{0,b}],\\ &= \mathrm{Tr}[HP_s],\end{aligned}$$

we find that (2.16) is equivalent to the following minimization problem

$$E^{\mathrm{PET}} = \inf_{\substack{P_s^2=P_s,\, P_s^*=P_s\\ P_{0,b}P_s=0,\, \mathrm{Tr}P_s=N_s}} \mathrm{Tr}[(I-P_{0,b})H(I-P_{0,b})P_s] + \mathrm{Tr}[HP_{0,b}]. \tag{2.18}$$

Given that $\mathrm{Tr}[HP_{0,b}]$ is a constant, we only need to focus on the first term $\mathrm{Tr}[(I - P_{0,b})H(I-P_{0,b})P_s]$. The matrix $(I-P_{0,b})H(I-P_{0,b})$, called the Huzinaga operator in quantum chemistry [16], is Hermitian and is identical to $H$ when restricted to the subspace $\mathcal{B}_0^\perp$. With some abuse of notation, $H|_{\mathcal{B}_0^\perp}$ can be diagonalized as

$$H|_{\mathcal{B}_0^\perp} = \hat{\Psi}\hat{\Lambda}\hat{\Psi}^*. \tag{2.19}$$

Since the dimension of $\mathcal{B}_0^\perp$ is $N-N_b$, $\hat{\Lambda} = \mathrm{diag}[\hat{\lambda}_1, \ldots, \hat{\lambda}_{N-N_b}] \in \mathbb{R}^{(N-N_b)\times(N-N_b)}$ is a diagonal matrix containing all the eigenvalues of $H|_{\mathcal{B}_0^\perp}$ ordered non-decreasingly, and $\hat{\Psi} \in \mathbb{C}^{N\times(N-N_b)}$ is given by orthogonal columns of a unitary matrix in the subspace $\mathcal{B}_0^\perp$. Then

$$\begin{aligned}\mathrm{Tr}[(I-P_{0,b})H(I-P_{0,b})P_s] &= \mathrm{Tr}[\hat{\Psi}\hat{\Lambda}\hat{\Psi}^*P_s] = \mathrm{Tr}[\hat{\Lambda}\hat{\Psi}^*P_s\hat{\Psi}]\\ &= \mathrm{Tr}[\hat{\Lambda}\hat{P}_s] = \sum_{i=1}^{N-N_b}\hat{\lambda}_i\hat{P}_{ii}.\end{aligned}$$

Here $\hat{P}_s$ is the matrix representation of $P_s$ with respect to the basis $\hat{\Psi}$ of the subspace $\mathcal{B}_0^\perp$.

Thus similar to the proof of Proposition 1, we arrive at the following minimization problem

$$E^{\mathrm{PET}} = \inf_{\substack{\hat{P}_s^2=\hat{P}_s,\, \hat{P}_s^*=\hat{P}_s\\ \mathrm{Tr}\hat{P}_s=N_s}} \mathrm{Tr}[\hat{\Lambda}\hat{P}_s] + \mathrm{Tr}[HP_{0,b}], \tag{2.20}$$

whose minimizer is given by

$$(\hat{P}_s)_{ij} = \begin{cases} 1, & \text{if } i=j \text{ and } i \le N_s,\\ 0, & \text{otherwise,}\end{cases} \tag{2.21}$$

and

$$P_s = \hat{\Psi}\hat{P}_s\hat{\Psi}^* = \Psi_s\Psi_s^*. \tag{2.22}$$

Here $\Psi_s$ are the first $N_s$ columns of $\hat{\Psi}$ corresponding to the lowest $N_s$ eigenvalues. □

Note that the eigenvalues $\{\hat{\lambda}_i\}$ are in general not the same as the original eigenvalues $\{\lambda_i\}$. Nonetheless, the trace $\sum_{i=1}^{N_s}\hat{\lambda}_i + \mathrm{Tr}[HP_{0,b}]$ yields a good approximation to the energy $E$ according to the proof of Proposition 2. Furthermore, even if $H_0$ and

$H$ satisfy the gap condition, $H|_{\mathcal{B}_0^\perp}$ does not necessarily satisfy the corresponding gap condition. Therefore we need to make the assumption explicit in the proposition.

Furthermore, when computing $\Psi_s$, we should note that the eigenpairs of $H|_{\mathcal{B}_0^\perp}$ and $(I-P_{0,b})H(I-P_{0,b})$ are not the same. More specifically, all the vectors $\Psi_{0,b}$ fall in the null space of $(I-P_{0,b})H(I-P_{0,b})$, and hence are legitimate eigenvectors corresponding to the eigenvalue 0. But this null space must be eliminated in the contribution to $P_s$ due to the orthogonality condition (1.3). This issue becomes noticeable when $\hat{\lambda}_{N_s} > 0$, and it would be incorrect to simply select the first $N_s$ eigenpairs of $(I-P_{0,b})H(I-P_{0,b})$. One practical way to get around this problem is to add a negative shift $c$, so that all the first $N_s$ eigenvalues of the matrix $(I - P_{0,b})(H + cI)(I - P_{0,b})$ become negative. This issue can also be automatically taken care of by applying the projector $I-P_{0,b}$ to the computed eigenvectors in an iterative solver, so that the computation is restricted to the subspace of interest $\mathcal{B}_0^\perp$.

REMARK 3. *The original formulation of PET [26] can be understood as a penalty formulation to implement the orthogonality constraint, i.e.*

$$E^{PET,\mu} = \inf_{\substack{P_s^2 = P_s,\, P_s^* = P_s \\ \mathrm{Tr}P_s = N_s}} \mathrm{Tr}[H(P_s + P_{0,b})] + \mu \mathrm{Tr}[P_{0,b}P_s]. \tag{2.23}$$

*This advantage of the penalty formulation is that the domain of $P_s$ has the same form as that in Proposition 1 but with a modified energy functional. The corresponding Euler-Lagrange equation is given by the eigenvalue problem for the matrix $H + \mu P_{0,b}$, and $P_s$ is the density matrix corresponding to the first $N_s$ eigenpairs. Therefore by selecting the penalty $\mu$ to be sufficiently large (in practice it is set to $10^6$ or larger), the orthogonality condition is approximately enforced.*

**3. Perturbative correction to PET for linear problems.** First, we would like to verify that PET is a consistent theory: when $H = H_0$ and $N_e = N_e^0$, for any choice of the reference $P_{0,b}$, the minimizers from (2.1) and (2.16) should yield the same density matrix. This is ensured by Proposition 4.

PROPOSITION 4 (Consistency of PET). *When $H = H_0$ and $N_e = N_e^0$, the solution to PET satisfies $P_s = P_{0,s}$.*

*Proof.* By the Courant-Fischer minimax theorem,

$$\hat{\lambda}_{N_s+1} = \max_{\substack{\dim(S)=N-N_e \\ S\subset\mathcal{B}_0^\perp}} \min_{u\in S\setminus\{0\}} \frac{u^* H|_{\mathcal{B}_0^\perp} u}{u^* u} \leq \max_{\dim(S)=N-N_e} \min_{u\in S\setminus\{0\}} \frac{u^* H u}{u^* u} = \lambda_{N_e+1}.$$

On the other hand, when $H = H_0$, all eigenvectors of $H$ corresponding to eigenvalues $\lambda_{N_e+1}$ and above are in the subspace $\mathcal{B}_0^\perp$, and hence $\hat{\lambda}_{N_s+1} \geq \lambda_{N_e+1}$. Therefore

$$\hat{\lambda}_{N_s+1} = \lambda_{N_e+1}.$$

Again using the Courant-Fischer minimax theorem we have

$$\hat{\lambda}_{N_s} \leq \lambda_{N_e}. \tag{3.1}$$

Hence the gap condition of $H$,*i.e.* , $\lambda_{N_e+1} - \lambda_{N_e} > 0$ implies that the gap condition for Proposition 2 holds, *i.e.*

$$\hat{\lambda}_{N_s+1} - \hat{\lambda}_{N_s} > 0.$$

Since the minimizer of PET is obtained from a constrained domain of the density matrix, we have

$$E = \inf_{\substack{P^2=P,\, P^*=P \\ \mathrm{Tr}P=N_e}} \mathrm{Tr}[H_0 P] \leq \inf_{\substack{P_s^2=P_s,\, P_s^*=P_s \\ \mathrm{Tr}P_s=N_s}} \mathrm{Tr}[H_0(P_s+P_{0,b})]. \tag{3.2}$$

where $P_s = P_{0,s}$ already achieves the minimum. By the uniqueness of the minimizer in Proposition 2, we have $P_s = P_{0,s}$. □

REMARK 5. *The proof of Proposition 4 is not entirely straightforward. This is mainly due to the fact that $P_{0,b}$ is obtained through some linear combination of eigenvectors of $H_0$ corresponding to the lowest $N_e$ eigenvalues. Hence $H$ and $P_{0,b}$ generally do not commute even when $H = H_0$. Nonetheless, the consistency of PET implies that PET is an in principle exact theory, given the proper choice of the reference projector $P_{0,b}$.*

In the following discussion, we would derive a perturbative correction to the density matrix when $H \approx H_0$. Unfortunately, standard perturbation analysis for eigenvalue problems do not apply directly given that PET solves two separate eigenvalue problems: one from $H_0$ and the other from $H|_{\mathcal{B}_0^\perp}$. In particular, the projector $P_{0,b}$, which determines the accuracy of PET, is evaluated from the reference problem $H_0$.

In order to bypass this difficulty, we show that PET can also be viewed as one eigenvalue problem but in a rotated basis, and we use standard perturbative analysis on the rotated problem to compute the rotation, the resulting perturbation is then rotated back to the original basis.

Let us split the set of vectors $\hat{\Psi}$ from the eigen-decomposition (2.19) as

$$\hat{\Psi} = [\Psi_s, \Psi_u],$$

where $\Psi_s$ corresponds the projector $P_s$ according to Proposition 2. Correspondingly the diagonal matrix $\hat{\Lambda}$ is split into the block diagonal form as

$$\hat{\Lambda} = \begin{bmatrix} \Lambda_s & 0 \\ 0 & \Lambda_u \end{bmatrix}.$$

Then, from $V$ we define a unitary $N \times N$ matrix

$$W := [\Psi_{0,b}, \Psi_s, \Psi_u], \tag{3.3}$$

and the matrix representation of $H$ with respect to the basis $W$, denoted by $H_W$, can be written as

$$\begin{aligned} H_W = W^* H W &= \begin{bmatrix} \Psi_{0,b}^* H \Psi_{0,b} & \Psi_{0,b}^* H \Psi_s & \Psi_{0,b}^* H \Psi_u \\ \Psi_s^* H \Psi_{0,b} & \Psi_s^* H \Psi_s & \Psi_s^* H \Psi_u \\ \Psi_u^* H \Psi_{0,b} & \Psi_u^* H \Psi_s & \Psi_u^* H \Psi_u \end{bmatrix}, \\ &= \begin{bmatrix} \Psi_{0,b}^* H \Psi_{0,b} & \Psi_{0,b}^* H \Psi_s & \Psi_{0,b}^* H \Psi_u \\ \Psi_s^* H \Psi_{0,b} & \Lambda_s & 0 \\ \Psi_u^* H \Psi_{0,b} & 0 & \Lambda_u \end{bmatrix}. \end{aligned}$$

In the second equality, we have used the fact that all columns of $\Psi_s, \Psi_u$ belong to $\mathcal{B}_0^\perp$, and consist of eigenvectors of $H|_{\mathcal{B}_0^\perp}$ associated with different sets of eigenvalues. Hence the inner product $\Psi_s^* H \Psi_u$ vanishes. Again we note that not all off-diagonal matrix blocks vanish even when $H = H_0$.

From this perspective, we find that PET makes two approximations: first, it discards the off-diagonal matrix blocks, so that

$$H_W \approx \begin{bmatrix} \Psi_{0,b}^* H \Psi_{0,b} & 0 & 0 \\ 0 & \Lambda_s & 0 \\ 0 & 0 & \Lambda_u \end{bmatrix},$$

and second, it replaces the block corresponding to the interactions within the bath by $\Psi_{0,b}^* H_0 \Psi_{0,b} = \Lambda_{0,b}$. The resulting matrix,

$$H_W^{\mathrm{PET}} = \begin{bmatrix} \Lambda_{0,b} & 0 & 0 \\ 0 & \Lambda_s & 0 \\ 0 & 0 & \Lambda_u \end{bmatrix},$$

is already diagonalized in the $W$-basis. Assume that the first $N_e$ eigenvalues of $H_W^{\mathrm{PET}}$ include all the diagonal entries of $\Lambda_{0,b}$ (according to Proposition 4, this is at least valid when $H = H_0$ and $N_e = N_e^0$), we find that the density matrix in the $W$-basis takes the block diagonal form

$$P_W^{\mathrm{PET}} = \begin{bmatrix} I_{N_b} & 0 & 0 \\ 0 & I_{N_s} & 0 \\ 0 & 0 & 0 \end{bmatrix}.$$

When rotated back to the standard basis, the density matrix becomes

$$P^{\mathrm{PET}} = W P_W^{\mathrm{PET}} W^* = \Psi_{0,b} \Psi_{0,b}^* + \Psi_s \Psi_s^* = P_s + P_{0,b},$$

which is the PET solution.

One advantage of the representation in the $W$-basis is that the density matrix $P_W^{\mathrm{PET}}$ can be concisely written using the Cauchy contour integral formulation as

$$P_W^{\mathrm{PET}} = \frac{1}{2\pi\imath} \oint_{\mathcal{C}} (zI - H_W^{\mathrm{PET}})^{-1} \, \mathrm{d}z. \tag{3.4}$$

Here $\mathcal{C}$ is a contour in the complex plane surrounding only the lowest $N_e$ eigenvalues of $H_W^{\mathrm{PET}}$.

The first order perturbative correction to PET is then given by the neglected off-diagonal matrix blocks $\Psi_s^* H \Psi_{0,b}$ and $\Psi_u^* H \Psi_{0,b}$, and the diagonal term involving $\Psi_{0,b}^* (H - H_0) \Psi_{0,b}$. The formula for the first order perturbation is given in Proposition 6.

PROPOSITION 6 (First order perturbation). *The first order perturbation to the density matrix from PET is given by*

$$\delta P = \delta\Psi_{0,b} \Psi_{0,b}^* + h.c. \tag{3.5}$$

*where $\delta\Psi_{0,b} \in \mathbb{C}^{N \times N_b}$ satisfies the equation*

$$Q \left( \lambda_{i;0,b} I - H \right) Q \delta\psi_{i;0,b} = Q(H\psi_{i;0,b}), \quad Q\delta\psi_{i;0,b} = \delta\psi_{i;0,b}. \tag{3.6}$$

*Here the projector $Q = I - (P_s + P_{0,b}) = \Psi_u \Psi_u^*$. $\lambda_{i;0,b}$ is the $i$-th diagonal element of $\Lambda_{0,b}$, and $\psi_{i;0,b}, \delta\psi_{i;0,b}$ are the $i$-th column of $\Psi_{0,b}, \delta\Psi_{0,b}$, respectively. h.c. stands for the Hermite conjugate of the first term.*

REMARK 7. *Following the previous notation we may define the subspace* $\mathcal{B} := span\{\Psi_s, \Psi_{0,b}\}$*, and* $Q$ *is the projector on the orthogonal complement subspace* $\mathcal{B}^\perp$*. Since* $\lambda_{0,b}$ *is separated from the spectrum of* $H|_{\mathcal{B}_0^\perp}$*, Eq.* (3.6) *has a unique solution in* $\mathcal{B}^\perp$*. Eq.* (3.5) *suggests that the first correction to the system part* $P_s$ *vanishes, and the correction only comes from the bath part* $P_{0,b}$*. Furthermore, the correction is traceless due to the condition* $\Psi_{0,b}^*\delta\Psi_{0,b} = 0$*. This means that the density matrix after the first order correction preserves the trace of the projector, which is* $N_e$*. In the context of KSDFT, this means that the first order correction preserves the number of electrons in the system.*

REMARK 8. *From Eq.* (3.6) *it may appear that the correction does not vanish even when* $H = H_0$*. However, note that* $H_0\psi_{i;0,b} \in \mathcal{B} := span\{\Psi_s, \Psi_{0,b}\}$*, we have* $QH_0\psi_{i;0,b} = 0$*, and hence the first order correction vanishes. This is consistent with Proposition 4.*

REMARK 9. *The perturbative correction requires the solution of* $N_b$ *linear equations to correct the projector from the bath. It seems that this diminishes the purpose of PET which reduces the number of eigenpairs to be computed from* $N_e$ *to* $N_s$ *from a practical perspective. Hence the advantage of the perturbative correction becomes more apparent in the nonlinear setup in section 4, where the perturbation only needs to be applied once after the self-consistency is achieved.*

*Proof.* Our strategy is to derive the first order perturbation in the $W$-basis, denoted by $\delta P_W$, and then obtain $\delta P$ according to $\delta P = W\delta P_W W^*$.

Let us first denote by

$$\delta H_W = \begin{bmatrix} \Psi_{0,b}^*\Delta H\Psi_{0,b} & \Psi_{0,b}^* H\Psi_s & \Psi_{0,b}^* H\Psi_u \\ \Psi_s^* H\Psi_{0,b} & 0 & 0 \\ \Psi_u^* H\Psi_{0,b} & 0 & 0 \end{bmatrix}$$

the neglected off-diagonal matrix blocks in PET, with $\Delta H = H - H_0$. $\delta H_W$ may not be small even when $H = H_0$, but its contribution to the density matrix must vanish according to Proposition 4, and hence can be treated perturbatively.

Let $P_W = P_W^{\mathrm{PET}} + \delta P_W$, setting $G_W(z) = (z - H_W)^{-1}$ and $G(z)_W^{\mathrm{PET}} = (z - H_W^{\mathrm{PET}})^{-1}$, we have the Dyson equation

$$G_W(z) = G_W^{\mathrm{PET}}(z) + G_W^{\mathrm{PET}}(z)\delta H_W G_W(z).$$

Thus using the Cauchy integral formulation we have that

$$\begin{aligned} \delta P_W =& P_W - P_W^{\mathrm{PET}} && (3.7)\\ =& \frac{1}{2\pi\imath}\oint_{\mathcal{C}} G_W(z) - G_W^{\mathrm{PET}}(z)\,\mathrm{d}z && (3.8)\\ =& \frac{1}{2\pi\imath}\oint_{\mathcal{C}} G_W^{\mathrm{PET}}(z)\delta H_W G_W(z)\,\mathrm{d}z && (3.9)\\ =& \frac{1}{2\pi\imath}\oint_{\mathcal{C}} (zI - H_W^{\mathrm{PET}})^{-1}\delta H_W (zI - H_W)^{-1}\,\mathrm{d}z. && (3.10) \end{aligned}$$

By setting $H_W \approx H_W^{\mathrm{PET}}$, the first order correction is

$$\delta P_W = \frac{1}{2\pi\imath}\oint_{\mathcal{C}} (zI - H_W^{\mathrm{PET}})^{-1}\delta H_W (zI - H_W^{\mathrm{PET}})^{-1}\,\mathrm{d}z.$$

Since $H_W^{\mathrm{PET}}$ is a diagonal matrix, $\delta P_W$ should have the same matrix sparsity pattern as $\delta H_W$, *i.e.*

$$\delta P_W = \begin{bmatrix} (\delta P_W)_{b,b} & (\delta P_W)_{b,s} & (\delta P_W)_{b,u} \\ (\delta P_W)_{s,b} & 0 & 0 \\ (\delta P_W)_{u,b} & 0 & 0 \end{bmatrix}.$$

First we compute

$$(\delta P_W)_{b,s} = \frac{1}{2\pi\imath} \oint_{\mathcal{C}} (zI - \Lambda_{0,b})^{-1} \Psi_{0,b}^* H \Psi_s (zI - \Lambda_s)^{-1} \,\mathrm{d}z.$$

Note that for any diagonal elements $\lambda_{i;0,b}, \lambda_{j;s}$ from $\Lambda_{0,b}, \Lambda_s$, respectively, they are both enclosed in the contour $\mathcal{C}$. If $\lambda_{i;0,b} \neq \lambda_{j;s}$, then

$$\begin{aligned} \frac{1}{2\pi\imath} \oint_{\mathcal{C}} (z - \lambda_{i;0,b})^{-1} (z - \lambda_{j;s})^{-1} \,\mathrm{d}z &= \frac{1}{2\pi\imath} \oint_{\mathcal{C}} \frac{(z - \lambda_{i;0,b})^{-1} - (z - \lambda_{j;s})^{-1}}{\lambda_{i;0,b} - \lambda_{j;s}} \,\mathrm{d}z \\ &= \frac{1 - 1}{\lambda_{i;0,b} - \lambda_{j;s}} = 0. \end{aligned}$$

On the other hand if $\lambda_{i;0,b} = \lambda_{j;s}$, we would obtain an integral of the form

$$\frac{1}{2\pi\imath} \oint_{\mathcal{C}} (z - \lambda_{i;0,b})^{-2} \,\mathrm{d}z,$$

which vanishes since the residue for the integrand is zero.

For the term

$$(\delta P_W)_{b,b} = \frac{1}{2\pi\imath} \oint_{\mathcal{C}} (zI - \Lambda_{0,b})^{-1} \Psi_{0,b}^* \Delta H \Psi_{0,b} (zI - \Lambda_{0,b})^{-1} \,\mathrm{d}z,$$

an analogous argument can be used to show that it vanishes.

This means that the matrix blocks $(\delta P_W)_{b,s}$, $(\delta P_W)_{s,b}$, and $(\delta P_W)_{b,b}$ vanish, and the only nonzero matrix blocks are $(\delta P_W)_{u,b}$ and its conjugate. Moreover,

$$\begin{aligned} (\delta P_W)_{u,b} =& \frac{1}{2\pi\imath} \oint_{\mathcal{C}} (zI - \Lambda_u)^{-1} \Psi_u^* H \Psi_{0,b} (zI - \Lambda_{0,b})^{-1} \,\mathrm{d}z, \\ =& \sum_i (\lambda_{i;0,b} - \Lambda_u)^{-1} \Psi_u^* H \psi_{i;0,b}. \end{aligned}$$

Back to the standard basis

$$\begin{aligned} \delta P =& \Psi_u \sum_i (\lambda_{i;0,b} - \Lambda_u)^{-1} \Psi_u^* H \psi_{i;0,b} \psi_{i;0,b}^* + \text{h.c.} \\ =& \left( \sum_i \delta\psi_{i;0,b} \psi_{i;0,b}^* \right) + \text{h.c.} \end{aligned}$$

Here

$$\delta\psi_{i;0,b} = \Psi_u (\lambda_{i;0,b} - \Lambda_u)^{-1} \Psi_u^* H \psi_{i;0,b}.$$

Using the projector $Q = \Psi_u \Psi_u^*$, we find that $\psi_{i;0,b}$ satisfies (3.6), and we prove the proposition. □

Finally, we summarize the perturbatively corrected PET in Algorithm 1.

**Algorithm 1** Perturbatively corrected projection based embedding theory for linear eigenvalue problems.

Input: $H$, $H_0$, $\Psi_{0,b}$, $\Psi_s$.
Output: $\delta\Psi_{0,b}, \delta P$.
1: Compute diagonal matrix $\Lambda_{0,b} = \Psi_{0,b}^* H_0 \Psi_{0,b}$.
2: Obtain the PET density matrix $P^{\mathrm{PET}} = \Psi_{0,b}\Psi_{0,b}^* + \Psi_s\Psi_s^*$.
3: Compute the right-hand side $R = (I - P^{\mathrm{PET}})H\Psi_{0,b}$.
4: Compute $\delta\Psi_{0,b}$ by solving (3.6).
5: Obtain the perturbation to the density matrix $\delta P = \delta\Psi_{0,b}\Psi_{0,b}^* + \Psi_{0,b}\delta\Psi_{0,b}^*$.

**4. PET for nonlinear problems.** In this section we generalize PET and the perturbative expansion to the nonlinear case as in KSDFT. First, define the energy functional

$$\mathcal{E}[P] = \mathrm{Tr}[PH_L] + E_{\mathrm{Hxc}}[P], \tag{4.1}$$

where $H_L$ is the linear part of the Hamiltonian, and is a given matrix derived from the discretized Laplacian operator and the electron-nuclei interaction potential. $E_{\mathrm{Hxc}}[P]$ consists of the Hartree, and exchange correlation energy, and is a nonlinear functional of the density matrix $P$. Moreover, all the information of the quantum system, including the atomic types and positions, is given by the electron-nuclei interaction in $H_L$. The ground state energy of KSDFT can be obtained from the following variational problem

$$E = \inf_{\substack{P^2 = P, P^* = P \\ \mathrm{Tr}P = N_e}} \mathcal{E}[P], \tag{4.2}$$

Analogous to Proposition 1, the corresponding Euler-Lagrange equation is

$$H[P]\Psi = (H_L + V_{\mathrm{Hxc}}[P])\Psi = \Psi\Lambda, \quad P = \Psi\Psi^*, \tag{4.3}$$

where $(\Psi, \Lambda)$ are the lowest $N_e$ eigenpairs of the nonlinear Hamiltonian $H[P]$, and the functional derivative $V_{\mathrm{Hxc}}[P] = \frac{\delta E_{\mathrm{Hxc}}[P]}{\delta P}$ is called the exchange-correlation potential. This is precisely (1.1). However, we remark that the procedure of taking the lowest $N_e$ eigenpairs, which is called the *aufbau* principle in electronic structure theories, is not always valid. The *aufbau* principle has been found to be violated for certain model energy functionals [25], but numerical experience indicates that it generally holds in the context of KSDFT calculations for real materials. In the discussion below, we always assume the counterpart to Proposition 1 holds for the nonlinear problems under consideration.

According to the discussion in section 2, the key ansatz of the PET is that for some reference system with a different linear part of the Hamiltonian $H_{0,L}$, we have evaluated the density matrix and computed the projector $P_{0,b}$. Then for the system of interest, PET evaluates the modified variational problem by restricting the domain of the density matrix as

$$E^{\mathrm{PET}} = \inf_{\substack{P_s^2 = P_s, P_s^* = P_s \\ P_{0,b}P_s = 0, \mathrm{Tr}P_s = N_s}} \mathcal{E}[P_s + P_{0,b}], \tag{4.4}$$

Analogous to Proposition 2, by assuming the corresponding *aufbau* principle, PET can be solved by the following nonlinear eigenvalue problem

$$H[P]|_{\mathcal{B}_0^\perp}\Psi_s := \Psi_s\Lambda_s, \quad P_s = \Psi_s\Psi_s^*, \quad P = P_s + P_{0,b}. \tag{4.5}$$

Here $(\Psi_s, \Lambda_s)$ are the lowest $N_s$ eigenpairs of the self-consistent Hamiltonian $H[P]|_{\mathcal{B}_0^\perp}$.

The first order perturbative correction to PET is entirely analogous to Proposition 6. According to Remark 9, the effectiveness of the perturbative approach mainly lies in the fact that it only needs to be applied once after (4.5) reaches self-consistency.

REMARK 10. *In [26] the Euler-Lagrange equation takes a slightly different form from* (4.5)*. The connection with the present formulation can be established by noting that the energy functional satisfies the identity*

$$\mathcal{E}[P_s + P_{0,b}] = \mathcal{E}[P_s] + \left(\mathcal{E}[P_s + P_{0,b}] - \mathcal{E}[P_s]\right).$$

*Then the Euler-Lagrange equation gives the Hamiltonian*

$$H_L + V_{\mathrm{Hxc}}[P_s] + (V_{\mathrm{Hxc}}[P_s + P_{0,b}] - V_{\mathrm{Hxc}}[P_s])$$

*restricted to the subspace $\mathcal{B}_0^\perp$. The term in the parenthesis, $V_{emb}(P_s) := (V_{\mathrm{Hxc}}[P_s + P_{0,b}] - V_{\mathrm{Hxc}}[P_s])$, is called the "embedding potential", which can be interpreted as an external potential imposed onto the system part from the bath. For instance, in the absence of the exchange-correlation, $V_{\mathrm{Hxc}} \equiv V_H$ is a linear mapping. Then $V_{emb} = V_H[P_{0,b}]$ is the Coulomb interaction solely due to the projector from the bath.*

**5. Evaluation of the reference projector.** The success of PET relies on a proper choice of the reference projector $P_{0,b}$. The suggestion from [26] is to compute a set of localized functions within the subspace $\mathrm{span}\{\Psi_0\}$ to evaluate $P_{0,b}$. For simplicity, we use the notation from the linear problem, but the procedure can be directly generalized to the nonlinear setup as well.

Simply speaking, for a class of matrices $H$ satisfying the gap condition, we may expect that the matrix elements of the density matrix $P$ decays rapidly along the off-diagonal direction. In the physics literature this is referred to as the "nearsightedness" principle [21, 29], and there is a rich literature studying the validity of such decay property (see *e.g.* [3, 1]). We further expect that there exists a unitary matrix $U \in \mathbb{C}^{N_e \times N_e}$, called a gauge matrix, so that each column of the rotated matrix $\Phi = \Psi U$ is localized, *i.e.* it concentrates on a small number of elements compared to the size of the vector $N$. We point out that efficient numerical algorithms have been developed to compute such gauge and the corresponding localized functions (see *e.g.* [10, 27, 8]). Once the localized functions are obtained, we may find localized functions associated with the index set for the bath $\mathcal{I}_b$ denoted by $\Psi_{0,b}$. To make the discussion self-contained, we briefly introduce the recently developed selected columns of the density matrix (SCDM) method [8] below as a simple and robust localization method to generate $P_{0,b}$. Other localization techniques can certainly be used as well.

The main idea of the SCDM procedure is that the localized function $\Phi$ are obtained directly from columns of the density matrix $P = \Psi\Psi^*$. However, picking $N_e$ random columns of $P$ may result in a poorly conditioned basis. In order to choose a well conditioned set of columns, denoted $\mathcal{C} = \{c_1, c_2, \ldots, c_{N_e}\}$, we may use a QR factorization with column pivoting (QRCP) procedure [12]. More specifically, we compute

$$\Psi^*\Pi = U \begin{bmatrix} R_1 & R_2 \end{bmatrix}, \tag{5.1}$$

where $\Pi$ is a permutation matrix so that $R_1$ is a well conditioned matrix. The set $\mathcal{C}$ is given by the union of the nonzero row indices of the first $N_e$ columns of the permutation matrix $\Pi$. The unitary matrix $U$ is the desired gauge matrix [8, 9], and $\Phi = \Psi U$ is a localized matrix. It can be seen that Eq. (5.1) directly leads to a QRCP factorization of $P$ as

$$P\Pi = \Psi\Psi^*\Pi = (\Psi U)\begin{bmatrix} R_1 & R_2 \end{bmatrix},$$

and $\Psi U$ is a matrix with orthogonal columns.

Let us apply the SCDM procedure to $H_0$ and its eigenfunctions $\Psi_0$. With some abuse of notation, from a pre-defined bath index set $\mathcal{I}_b \subset \{1, \ldots, N\}$, we may associate the $i$-th column of $\Phi_0$ to the bath degrees of freedom if the $i$-th element of $\mathcal{C}$ is in $\mathcal{I}_b$. These selected vectors, denoted by $\Phi_{0,b}$ form the reference projector $P_{0,b}$. Finally, the condition (2.14) can be satisfied by solving the following eigenvalue problem

$$\Phi_{0,b}^* H_0 \Phi_{0,b} C_{0,b} = C_{0,b}\Lambda_{0,b}, \tag{5.2}$$

and then $\Psi_{0,b} = \Phi_{0,b}C_{0,b}$. We summarize the procedure for computing the $\Psi_{0,b}$ in Algorithm 2.

**Algorithm 2** Using the SCDM algorithm for constructing the reference projector.

Input: $H_0$, $\Psi_0$, $\mathcal{I}_b$, $N_e^0$.
Output: $\Psi_{0,b}$.
1: Perform QRCP for $\Psi_0^*$: $\Psi_0^*\Pi = U\begin{bmatrix} R_1 & R_2 \end{bmatrix}$. The set $\mathcal{C}$ is given by the union of the nonzero row indices of the first $N_e^0$ columns of the permutation matrix $\Pi$.
2: Compute $\Phi_0 = \Psi_0 U$. Form a submatrix $\Phi_{0,b} := [\varphi_{i;0}]_{\mathcal{C}_i \in \mathcal{I}_b}$, where $\varphi_{i;0}$ is the $i$-th column of $\Phi_0$.
3: Solve the eigenvalue problem (5.2), and compute $\Psi_{0,b} = \Phi_{0,b}C_{0,b}$.

**6. Numerical Examples.** We present several examples to demonstrate the effectiveness of the PET method and the perturbation scheme. The numerical tests were coded in Matlab 2017b. For the solution of KSDFT in the nonlinear case, we have implemented PET and the perturbation correction in the KSSOLV [34] software package. All calculations are performed run in a dual socket server with Intel Xeon E5-2670 CPU's and 386 Gb of RAM.

**6.1. Linear Case.** We first consider a simple Hamiltonian in 1D with zero Dirichlet boundary conditions:

$$H_0 = -\frac{1}{2}\frac{d^2}{dx^2} + V_0(x), \quad V_0(x) := \sum_{i=1}^{3} -40e^{-100(x-\tilde{x}_i)^2}, \quad x \in [-1, 1]. \tag{6.1}$$

Here the centers of the Gaussians $\tilde{x} = (-0.5, 0, 0.5)^T$. The 1D Laplacian is discretized with a standard 3- point stencil finite difference scheme with 512 grid points.

For the reference problem, we evaluate the 3 eigenfunctions corresponding to the lowest 3 eigenvalues. As shown in Fig. 6.2, the eigenvectors $\Psi_0$ are indeed delocalized across the entire interval $[-1, 1]$. After applying the SCDM algorithm (see Alg. 2), the resulting orbitals $\Phi_0$ become much more localized as shown in Fig. 6.2.

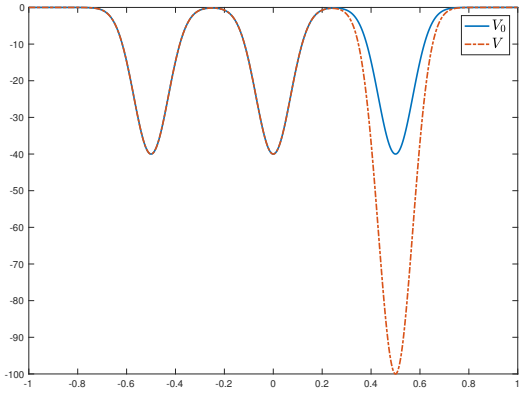


Fig. 6.1: Potential for both $H_0$ and $H$.

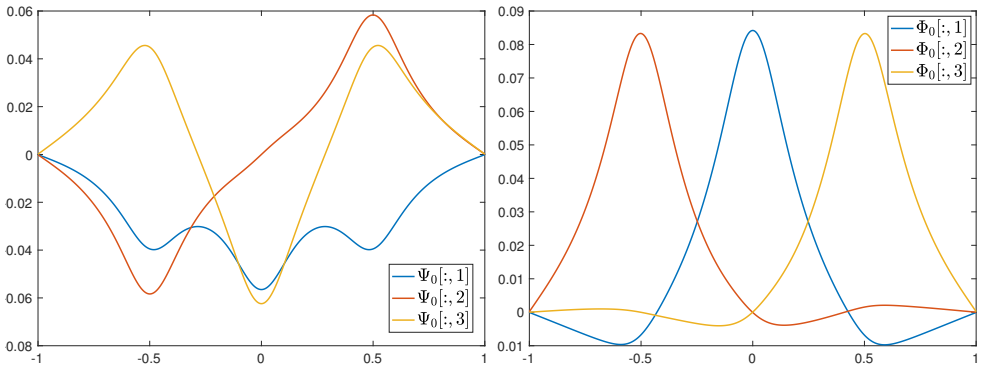


Fig. 6.2: *Left*: First 3 delocalized orbitals (columns of $\Psi_0$); *right*: first 3 localized orbitals (columns of $\Phi_0$).

We define the new Hamiltonian by changing the height of the last Gaussian function as

$$H = -\frac{1}{2}\frac{d^2}{dx^2} + V(x), \quad V(x) := \sum_{i=1}^{2} -40e^{-100(x-\tilde{x}_i)^2} - 100e^{-100(x-\tilde{x}_3)^2}, \tag{6.2}$$

We observe that two columns in $\Phi_0$ are localized far from the modified Gaussian, and we consider them as the bath orbitals. We set $\mathcal{I}_b = \{1, \ldots, 340\}$ and thus $\Phi_{0,b} = [\Phi_0[:,1], \Phi_0[:,2]]$. Along the same line, we set $\mathcal{I}_s = \{1, \ldots, 512\} - \mathcal{I}_b$. We then compute the linear PET problem to obtain $\Psi_s$, and we build PET density matrix shown in Fig. 6.3, which agrees well with the exact density matrix, and is accurate up to 3 digits in relative error. Furthermore, the error is mostly localized around the third Gaussian function as one would expect. The relative error of the energy is $1.42e-03$. We find it remarkable that for such a small system, the solution from PET is already very accurate despite the strong overlap of the system and bath orbitals.

Finally, we use Alg. 1 to compute the perturbed density matrix, which is more accurate than PET density matrix without the perturbation as depicted in Fig. 6.4.

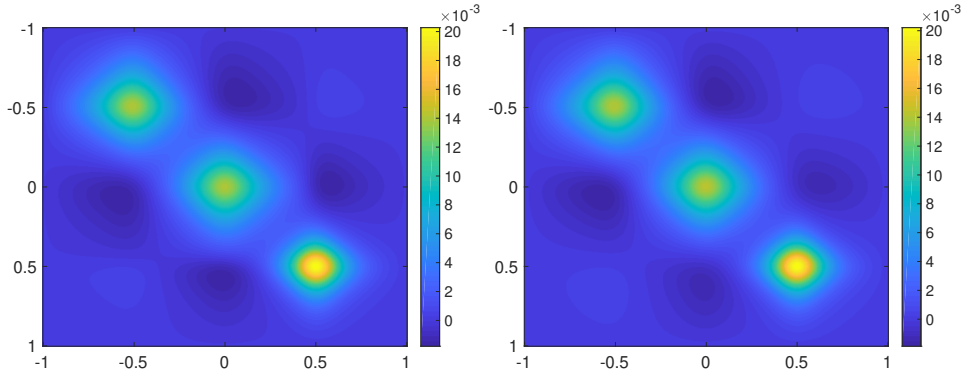


Fig. 6.3: (*left*) Exact density matrix; (*right*) PET density matrix

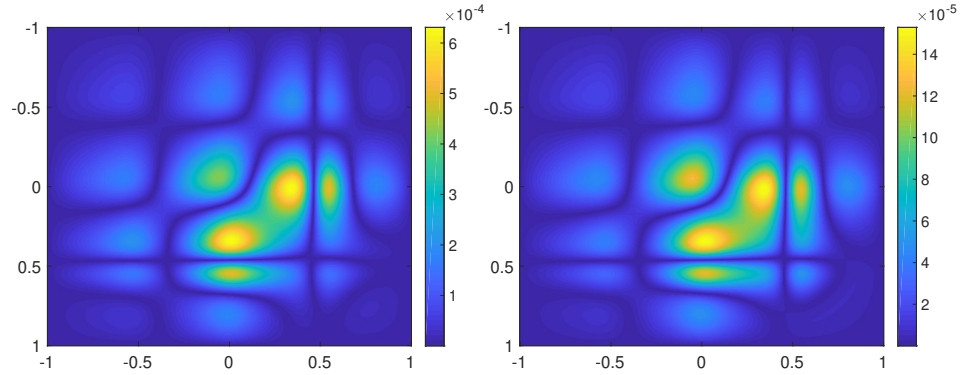


Fig. 6.4: Error of the density matrix with respect to the reference answer: (*left*) PET density matrix; (*right*) PET density matrix plus perturbation.

We can observe how the perturbation decreases the error in the density matrix by taking a look at the charge density, $\rho = \mathrm{diag}(P)$ in Fig. 6.5. In addition, the accuracy of the energy is improved, with its relative error reduced from $1.42e{-}03$ au to $1.01e{-}04$ au. If we increase the bath size from 1 to 2, the accuracy of the energy is improved further to $7.15e{-}05$ au and $2.12e{-}05$ au, without and with the perturbative correction, respectively.

**6.2. Nonlinear Case.** For KSDFT calculations, we modified the KSSOLV software package [34] to solve the PET equations (4.5) and to obtain the perturbation correction. KSSOLV uses a pseudo spectral discretization with the plane wave set. All the operators, including Hamiltonian and projection operators, are efficiently implemented in a matrix-free fashion. Within each self-consistent field iteration, we use the locally optimal block preconditioned conjugate gradient method (LOBPCG) [20] to solve the linear eigenvalue problems. For the perturbative correction, we use the GMRES [30] method with a preconditioner of the type [32] implemented via fast Fourier transforms (FFTs).

**6.2.1. Silane.** We first consider a simple molecule, silane ($SiH_4$), whose charge density in shown in Fig. 6.6 and we performed three different numerical experiments to showcase the accuracy of the method. Our reference system is the silane molecule

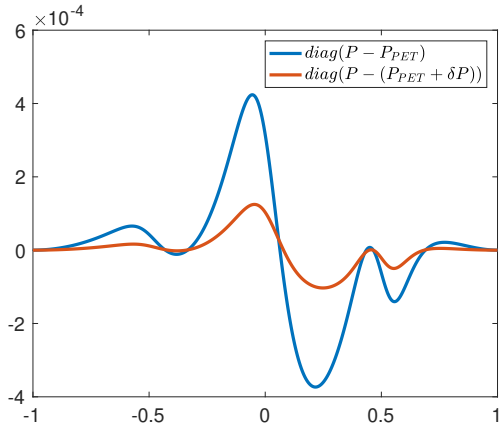


Fig. 6.5: Relative error of the charge density using PET density matrix and the perturbed PET density matrix.

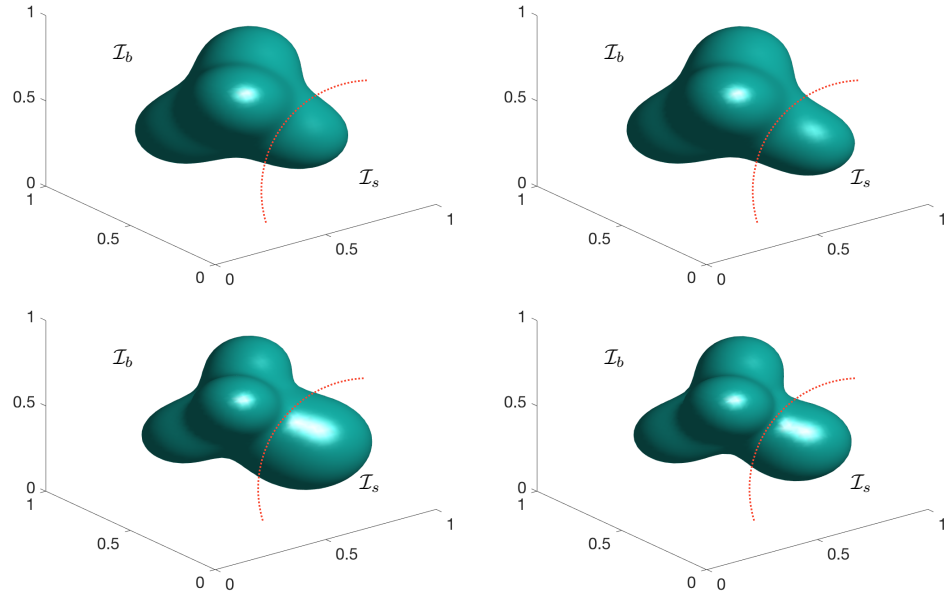


Fig. 6.6: (*top-left*) Electron charge density of the silane molecule, (*top-right*) electron charge density of the $SiH_4$ molecule with one hydrogen bond elongated, (*bottom-left*) electron charge density of $SiH_3Cl$, and, (*bottom-right*) electron charge density of $SiH_3F$.

from an equilibrium configuration. The bath-system partition is shown in Fig. 6.6, in which we can observe that we fixed three orbitals as the bath, indicated by $\mathcal{I}_b$, and the system part, which is delimited by a pointed red line is considered as the forth orbital indicated by $\mathcal{I}_s$. We performed three different modifications to the atom associated with the fourth orbital:

| Experiment | $\frac{\|\|P-P_{\text{PET}}\|\|}{\|\|P\|\|}$ | $\frac{\|\|P-P_{pert}\|\|}{\|\|P\|\|}$ | $\frac{\|\|\rho_{\text{PET}}-\rho\|\|}{\|\|\rho\|\|}$ | $\frac{\|\|\rho_{pert}-\rho\|\|}{\|\|\rho\|\|}$ |
|---|---|---|---|---|
| Elongated | 6.03e-02 | 1.40e-02 | 1.24e-02 | 8.00e-03 |
| $SiH_3Cl$ | 7.70e-02 | 1.74e-02 | 1.51e-02 | 6.71e-03 |
| $SiH_3F$ | 9.12e-02 | 2.09e-02 | 6.64e-03 | 4.72e-03 |

Table 6.1: Errors of the density matrices and electron densities for the different perturbation of the $SiH_4$ molecule.

| Experiment | $E - E_{\text{PET}}$ | $E - E_{\text{pert}}$ | $F - F_{\text{PET}}$ | $F - F_{\text{pert}}$ |
|---|---|---|---|---|
| Elongated | 5.98e-03 | 2.29e-04 | 1.51e-02 | 1.33e-03 |
| $SiH_3Cl$ | 1.84e-02 | 1.94e-03 | 1.89e-02 | 2.72e-03 |
| $SiH_3F$ | 1.66e-02 | 1.33e-03 | 9.29e-05 | 1.13e-03 |

Table 6.2: Errors for the different perturbation of the $SiH_4$ molecule.

- we elongate one hydrogen bond by 25%,
- we replace a hydrogen atom by a chlorine atom (Cl),
- we replace a hydrogen atom by a fluorine atom (F).

Note that in the latter two examples, the number of valence orbitals in the reference system is 4, which is different from in the perturbed system, which are 7. Hence the perturbation introduced by the atom substitution is very large, especially compared to the small size of the molecule under study here.

We compare the results from PET and the perturbed PET against a reference solution obtained directly by solving the system in KSSOLV. In particular, we examine the relative error of the density matrices, the relative error of the charge density, the absolute error of the energy, and the absolute error of the atomic force at the modified location. All results are reported in the atomic unit. In particular, the unit of the energy is Hartree, and the unit of the atomic force is Hartree / Bohr. In this case, the energy for PET was computed using the functional in (4.4). For the perturbed solution, we used *i.e.* $\text{Tr}[H_L(P^{PET} + \delta P)] + E_{\text{Hxc}}[P^{PET} + \delta P]$.

We point out that we can compute the atomic forces for the PET solution using the Hellmann-Feynman formula, which is due to the fact that the solution satisfies a variational principle. However, for the perturbation, the resulting approximation does not satisfy any variational principle, thus we use an expensive finite difference approach to compute the forces. We use an standard second order finite difference scheme to approximate the derivate of the force for both PET and perturbed solutions at the modified atom.

The results for each of the experiments are shown in Tables 6.1 and 6.2. We can observe that the perturbation effectively reduces the error of the density matrix, the electron density, the energy and atomic force. The only exception is the force of $SiH_3F$, which becomes coincidentally accurate for the PET, but the error after applying the perturbation theory is still around $1e-3$ au. Even for such a small system, after applying the perturbation formula, the error of the energy and force already reaches chemical accuracy.

**6.2.2. Benzene.** In this example we show the performance of the method for a benzene molecule ($C_6H_6$), whose charge density is shown in Fig. 6.7 (*left*). We substitute one of hydrogen atoms by a fluorine atom, and the resulting charge density is shown in Fig. 6.7 (*right*). In this case, the benzene molecule has a total of 15

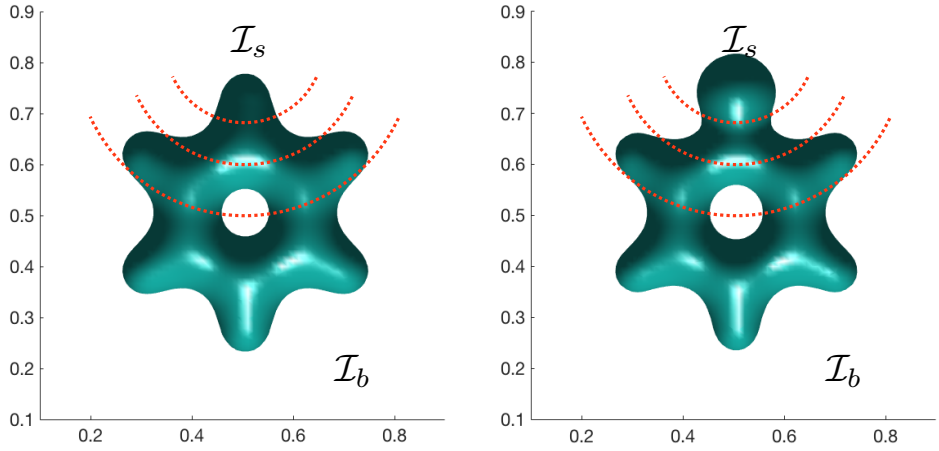


Fig. 6.7: Electron charge density for the benzene molecule (*left*), and the benzene molecule with an hydrogen atom replace by a fluorine (*right*).

| $N_s$ | $\frac{\|\|P-P_{\text{PET}}\|\|}{\|\|P\|\|}$ | $\frac{\|\|P-P_{\text{pert}}\|\|}{\|\|P\|\|}$ | $\frac{\|\|\rho_{PET}-\rho\|\|}{\|\|\rho\|\|}$ | $\frac{\|\|\rho_{pert}-\rho\|\|}{\|\|\rho\|\|}$ |
|---|---|---|---|---|
| 1 | 9.41e-02 | 5.65e-02 | 1.36e-02 | 2.04e-02 |
| 3 | 6.32e-02 | 1.93e-02 | 5.56e-03 | 6.70e-03 |
| 5 | 6.46e-02 | 1.61e-02 | 4.41e-03 | 3.27e-03 |
| 7 | 5.04e-02 | 1.13e-02 | 2.93e-03 | 1.72e-03 |
| 9 | 2.98e-02 | 4.12e-03 | 1.56e-03 | 1.32e-03 |

Table 6.3: Errors of the density matrix and electron density for the benzene molecule for different bath (and system) sizes.

valence orbitals, and the bath orbitals are the localized orbitals whose centroids are outside a sphere centered in the atom that is replaced. In this case, to generate the Tables 6.3 and 6.4 we compute the location of the centroids using the pivots of in the SCDM algorithm. Then we compute the distance of the modified atom to all centroids, taking in account the periodicity of the supercell. We label the orbitals associated to the closest $N_s$ centroids as the system orbitals, and the rest $N_b$ orbitals as the bath orbitals. The different partitions are depicted in Fig. 6.7, for $N_s = 1, 4$ and 6, in which the segmented red line indicates the boundary between the bath and system partitions. Tables 6.3 and 6.4 show the errors of the density matrix and the electron density, as well as the energy and the atomic force systematically decrease as the bath size increases. When the bath size is 7, the error of the energy and force after perturbative correction is already below the chemical accuracy and is as small as $1.02e-04$ and $4.17e-04$ au, respectively.

**6.2.3. Anthracene.** Finally we test our algorithm with the anthracene molecule ($C_{14}H_{10}$), which is composed of 3 benzene rings positioned longitudinally. Following the same procedure as with the benzene molecule, we compute the solution to the Kohn-Sham equations, whose charge density is shown in Fig. 6.8 , and we replace one hydrogen atom in one of the extremal rings by a fluorine atom (Fig. 6.8 *(right)*). From the total 33 orbitals for the anthracene, we define the bath orbitals by the localized

| $N_s$ | $E - E_{\mathrm{PET}}$ | $E - E_{\mathrm{pert}}$ | $F - F_{\mathrm{PET}}$ | $F - F_{\mathrm{pert}}$ |
|---|---|---|---|---|
| 1 | 4.05e-02 | 1.33e-02 | 2.69e-02 | 3.16e-02 |
| 3 | 1.87e-02 | 3.42e-03 | 1.73e-02 | 9.98e-03 |
| 5 | 1.20e-02 | 1.78e-03 | 4.24e-03 | 6.78e-03 |
| 7 | 7.89e-03 | 1.02e-04 | 3.73e-03 | 4.17e-04 |
| 9 | 3.02e-03 | 3.16e-05 | 4.05e-03 | 3.31e-04 |
| 11 | 2.81e-03 | 6.71e-05 | 3.68e-03 | 3.50e-04 |

Table 6.4: Errors of the energy and forces for the benzene molecule for different bath (and system) sizes.

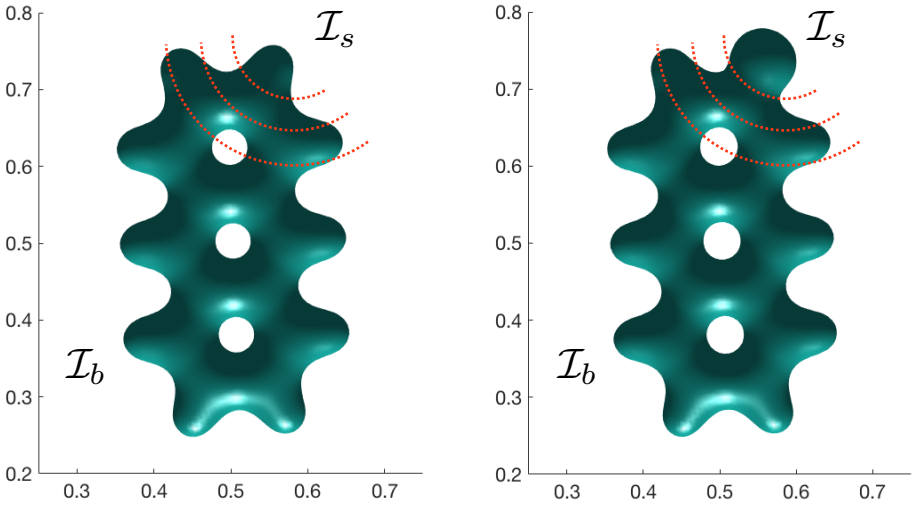


Fig. 6.8: Electron charge density for the anthracene molecule (*left*), and the anthracene molecule with an hydrogen atom replaced by a fluorine (*right*).

orbitals whose centroids lye outside a sphere centered at the replaced atom. The partitions for $N_s = 1, 4$, and 6 are depicted in Fig. 6.8, where the different segmented red lines indicate the boundary between the two partitions, in which they are denoted by $\mathcal{I}_b$ and $\mathcal{I}_s$, for the bath and for the system respectively.

We compute the PET approximation and its perturbation for several different bath sizes as shown in Table 6.5. From Table 6.5 we can clearly observe the error of all quantities decrease systematically with respect to the increase of the system size, and the perturbation method significantly increases the accuracy over the PET results. In particular, when the bath size is 7, chemical accuracy is achieved after the perturbative correction is applied.

**7. Conclusion.** We have studied the recently developed projection based embedding theory (PET) from a mathematical perspective. Viewed as a method to approximately solve eigenvalue problems, PET solves a deflated eigenvalue problem by taking into account the knowledge from a related reference system. This deflated eigenvalue problem can be derived from the Euler-Lagrange equation of a standard energy minimization procedure with respect to the density matrices, by with a non-standard constraint on the domain. From this perspective, the original formulation

| $N_s$ | $\frac{\|\|P-P_{\mathrm{PET}}\|\|}{\|\|P\|\|}$ | $\frac{\|\|P-P_{\mathrm{pert}}\|\|}{\|\|P\|\|}$ | $\frac{\|\|\rho_{PET}-\rho\|\|}{\|\|\rho\|\|}$ | $\frac{\|\|\rho_{pert}-\rho\|\|}{\|\|\rho\|\|}$ |
|---|---|---|---|---|
| 1 | 8.65e-02 | 4.85e-02 | 1.59e-02 | 1.50e-02 |
| 3 | 6.10e-02 | 2.07e-02 | 5.47e-03 | 7.18e-03 |
| 5 | 5.01e-02 | 3.33e-02 | 3.24e-03 | 3.25e-03 |
| 7 | 4.42e-02 | 1.61e-02 | 2.47e-03 | 1.91e-03 |
| 9 | 3.31e-02 | 6.33e-03 | 1.13e-03 | 9.75e-04 |
| 11 | 2.88e-02 | 6.31e-03 | 1.12e-03 | 9.04e-04 |
| 13 | 2.86e-02 | 6.63e-03 | 1.03e-03 | 7.90e-04 |
| 15 | 1.83e-02 | 4.40e-03 | 6.73e-04 | 5.68e-04 |
| 19 | 1.73e-02 | 3.12e-03 | 5.23e-04 | 4.13e-04 |

Table 6.5: Errors for the anthracene molecule for different bath (and system) sizes.

| $N_s$ | $E - E_{\mathrm{PET}}$ | $E - E_{\mathrm{pert}}$ | $F - F_{\mathrm{PET}}$ | $F - F_{\mathrm{pert}}$ |
|---|---|---|---|---|
| 1 | 4.06e-02 | 1.33e-02 | 2.69e-02 | 3.16e-02 |
| 3 | 1.87e-02 | 3.42e-03 | 1.73e-02 | 9.98e-03 |
| 5 | 1.10e-02 | 1.97e-03 | 7.72e-03 | 6.78e-03 |
| 7 | 8.18e-03 | 2.02e-04 | 3.73e-03 | 9.79e-04 |
| 9 | 4.02e-03 | 3.16e-05 | 4.05e-03 | 3.31e-04 |
| 11 | 2.74e-03 | 2.53e-05 | 4.42e-03 | 2.64e-04 |
| 13 | 2.26e-03 | 6.35e-05 | 4.53e-03 | 2.15e-04 |
| 15 | 9.70e-04 | 1.15e-05 | 1.84e-03 | 2.83e-04 |
| 19 | 7.34e-04 | 5.16e-06 | 1.62e-03 | 1.02e-04 |

Table 6.6: Errors of the energy and forces for the anthracene molecule for different bath (and system) sizes.

of PET can be seen as a penalty method for imposing the constraint. Numerical examples for linear problems as well as nonlinear problems from Kohn-Sham density functional theory calculations indicate that PET can yield accurate approximation to the density matrix, energy and atomic forces. In order to further improve the accuracy of PET, we developed a first order perturbation formula. We find that with the help of the perturbative treatment, PET can achieve chemical accuracy even for systems of relatively small sizes.

There are several immediate directions for future work. First, we have studied PET when the system and bath are treated using the same level of theory. From a physics perspective, it is more attractive to consider the case when the system part is treated with a more accurate theory than KSDFT with semi-local exchange-correlation functionals. In particular, it would be interesting to understand PET when the system part is treated using KSDFT with nonlocal functionals such as hybrid functionals, or wavefunction theories such as the coupled cluster (CC) method. It is also interesting to explore the PET in the context of solving time-dependent problems. Second, PET provides a size consistent alternative for many methods in quantum physics and chemistry to be applied to solid state systems. Some directions have already been pursued recently for using PET in the context of periodic systems [24, 6]. Third, the computation of the atomic force in PET is currently performed using the finite difference formula, which is expensive in practice. It would be desirable to develop a method with cost comparable to the Hellmann-Feynman method but

without significant sacrifice of the accuracy. Finally, we believe that the asymptotic convergence property of PET is still dictated by the nearsightedness principle for systems satisfying the gap condition, but numerical results indicate that PET already achieves high accuracy even for system sizes that are well below the prediction from localization theories. Therefore it is worthwhile to further study the convergence properties of PET, as well as to perform further comparison with linear scaling type methods.

**Acknowledgment.** This work was partially supported by the Department of Energy under Grant No. DE-SC0017867, No. DE-AC02-05CH11231, the SciDAC program, and by the Air Force Office of Scientific Research under award number FA9550-18-1-0095 (L. L. and L. Z.-N.), and by the National Science Foundation under Grant No. DMS-1652330 (L. L.). We thank the Berkeley Research Computing (BRC) program at the University of California, Berkeley for making computational resources available. We thank Garnet Chan and Frederick Manby for discussions, and Joonho Lee for valuable suggestions and careful reading of the manuscript.

REFERENCES

[1] M. Benzi, P. Boito, and N. Razouk, *Decay properties of spectral projectors with applications to electronic structure*, SIAM Rev., 55 (2013), pp. 3–64.

[2] J. Bernholc, N. O. Lipari, and S. T. Pantelides, *Self-consistent method for point defects in semiconductors: Application to the vacancy in silicon*, Phys. Rev. Lett., 41 (1978), p. 895.

[3] C. Brouder, G. Panati, M. Calandra, C. Mourougane, and N. Marzari, *Exponential localization of Wannier functions in insulators*, Phys. Rev. Lett., 98 (2007), p. 046402.

[4] H. Chen and C. Ortner, *QM/MM methods for crystalline defects. Part 2: Consistent energy and force-mixing*, arXiv:1509.06627, (2015).

[5] W. Chibani, X. Ren, M. Scheffler, and P. Rinke, *Self-consistent Green's function embedding for advanced electronic structure methods based on a dynamical mean-field concept*, Phys. Rev. B, 93 (2016), p. 165106.

[6] D. V. Chulhai and J. D. Goodpaster, *Projection-based correlated wave function in density functional theory embedding for periodic systems*, J. Chem. Theory Comput., 14 (2018), pp. 1928–1942.

[7] P. Cortona, *Self-consistently determined properties of solids without band-structure calculations*, Phys. Rev. B, 44 (1991), p. 8454.

[8] A. Damle, L. Lin, and L. Ying, *Compressed representation of Kohn–Sham orbitals via selected columns of the density matrix*, J. Chem. Theory Comput., 11 (2015), pp. 1463–1469.

[9] A. Damle, L. Lin, and L. Ying, *Accelerating selected columns of the density matrix computations via approximate column selection*, SIAM J. Sci. Comput., 39 (2017), p. 1178.

[10] J. M. Foster and S. F. Boys, *Canonical configurational interaction procedure*, Rev. Mod. Phys., 32 (1960), p. 300.

[11] C.J. García-Cervera, J. Lu, and W. E, *Asymptotics-based sub-linear scaling algorithms and application to the study of the electronic structure of materials*, Commun. Math. Sci., 5 (2007), pp. 999–1024.

[12] G. H. Golub and C. F. Van Loan, *Matrix computations*, Johns Hopkins Univ. Press, Baltimore, fourth ed., 2013.

[13] J. D. Goodpaster, N. Ananth, F. R. Manby, and T. F. Miller III, *Exact nonadditive kinetic potentials for embedded density functional theory*, J. Chem. Phys., 133 (2010), p. 084103.

[14] P. Hohenberg and W. Kohn, *Inhomogeneous electron gas*, Phys. Rev., 136 (1964), pp. B864–B871.

[15] C. Huang, M. Pavone, and E. A. Carter, *Quantum mechanical embedding theory based on a unique embedding potential*, J. Chem. Phys., 134 (2011), p. 154110.

[16] S. Huzinaga and A. A. Cantu, *Theory of separability of many-electron systems*, J. Chem. Phys., 55 (1971), pp. 5543–5549.

[17] A. A. Kananenka, E. Gull, and D. Zgid, *Systematically improvable multiscale solver for correlated electron systems*, Phys. Rev. B, 91 (2015), p. 121111.

[18] P. J. Kelly and R. Car, *Green's-matrix calculation of total energies of point defects in silicon*, Phys. Rev. B, 45 (1992), p. 6543.
[19] G. Knizia and G. K.-L. Chan, *Density matrix embedding: A strong-coupling quantum embedding theory*, J. Chem. Theory Comput., 9 (2013), pp. 1428–1432.
[20] A. V. Knyazev, *Toward the optimal preconditioned eigensolver: Locally optimal block preconditioned conjugate gradient method*, SIAM J. Sci. Comp., 23 (2001), pp. 517–541.
[21] W. Kohn, *Density functional and density matrix method scaling linearly with the number of atoms*, Phys. Rev. Lett., 76 (1996), pp. 3168–3171.
[22] W. Kohn and L. Sham, *Self-consistent equations including exchange and correlation effects*, Phys. Rev., 140 (1965), pp. A1133–A1138.
[23] X. Li, L. Lin, and J. Lu, *PEXSI-$\sigma$: A Green's function embedding method for Kohn-Sham density functional theory*, Ann. Math. Sci. Appl. in press, (2017).
[24] F. Libisch, M. Marsman, J. Burgdörfer, and G. Kresse, *Embedding for bulk systems using localized atomic orbitals*, J. Chem. Phys., 147 (2017), p. 034110.
[25] X. Liu, Z. Wen, X. Wang, M. Ulbrich, and Y. Yuan, *On the analysis of the discretized Kohn–Sham density functional theory*, SIAM J. Numer. Anal., 53 (2015), pp. 1758–1785.
[26] F. R. Manby, M. Stella, J. D. Goodpaster, and T. F. Miller III, *A simple, exact density-functional-theory embedding scheme*, J. Chem. Theory Comput., 8 (2012), pp. 2564–2568.
[27] N. Marzari and D. Vanderbilt, *Maximally localized generalized Wannier functions for composite energy bands*, Phys. Rev. B, 56 (1997), p. 12847.
[28] T. Nguyen, A. A. Kananenka, and D. Zgid, *Rigorous ab initio quantum embedding for quantum chemistry using Green's function theory: Screened interaction, nonlocal self-energy relaxation, orbital basis, and chemical accuracy*, J. Chem. Theory Comput., (2016).
[29] E. Prodan and W. Kohn, *Nearsightedness of electronic matter*, Proc. Natl. Acad. Sci., 102 (2005), pp. 11635–11638.
[30] Y. Saad and M. H. Schultz, *GMRES: A generalized minimal residual algorithm for solving nonsymmetric linear systems*, SIAM J. Sci. Stat. Comput., 7 (1986), pp. 856–869.
[31] Q. Sun and G. K.-L. Chan, *Quantum embedding theories*, Acc. Chem. Res., 49 (2016), pp. 2705–2712.
[32] M.P. Teter, M.C. Payne, and D.C. Allan, *Solution of Schrödinger's equation for large systems*, Phys. Rev. B, 40 (1989), p. 12255.
[33] A. R. Williams, P. J. Feibelman, and N. D. Lang, *Green's-function methods for electronic-structure calculations*, Phys. Rev. B, 26 (1982), p. 5433.
[34] C. Yang, J. C. Meza, B. Lee, and L. W. Wang, *KSSOLV–a MATLAB toolbox for solving the Kohn–Sham equations*, ACM Trans. Math. Software, 36 (2009), p. 10.
[35] R. Zeller and P. H. Dederichs, *Electronic Structure of Impurities in Cu, Calculated Self-Consistently by Korringa-Kohn-Rostoker Green's-Function Method*, Phys. Rev. Lett., 42 (1979), p. 1713.
[36] D. Zgid and G. K.-L. Chan, *Dynamical mean-field theory from a quantum chemical perspective*, J. Chem. Phys., 134 (2011), p. 094115.